Mathematical Analysis of Efficiencies in Hydraulic Pumps for Automatic Transmissions

N. YOSHIDA Y. INAGUMA

This paper deals with a mathematical analysis of pump efficiencies in an internal gear and a balanced vane pumps. They are commonly used in current automatic transmissions including a continuously variable transmission. For these pumps, the influence of oil temperature as well as pump-operating pressures and pump speeds is clarified by using mathematical models taking oil temperature into consideration, which are constructed on the basis of actual measured flow and torque data under various pump-operating conditions. For fuel economy in a vehicle, because the pump should be operated under conditions to obtain higher pump efficiencies, it is very important to understand the relationship between the pump efficiencies and the pump-operating conditions. This paper reveals that the mathematical models representing the leakage flow and friction torque characteristics accurately is helpful to investigate the pump efficiencies as well as the flow and torque performance under various pump-operating conditions. As a result, the overall efficiency decreases at extremely low and high oil temperatures. In the internal gear and the balanced vane pumps tested in this work, the region with a higher overall efficiency lies around an oil temperature of 80℃.

***Key Words**: Fluid power system, hydraulic pump, pump efficiencies, mathematical model, operating condition, oil temperature*

1. Introduction

In an automatic transmission (AT) and a continuously variable transmission (CVT), an internal gear pump has conventionally been used [1]. These days, a balanced vane pump with a fixed-displacement is also used for CVT operated at the maximum pressure of 5 MPa because of its good volumetric efficiency [2, 3]. For an improvement in the efficiency of these transmissions, it is important to reduce energy consumption of the pump [1, 4]. Actually, the pump is operated across a broad range of oil temperatures as well as pressures and pump speeds in the vehicle. Because such pump-operating conditions affect significantly the pump efficiencies, it is very important to understand how the pump efficiencies depend on the pump-operating conditions.

Although the volumetric, the mechanical and the overall efficiencies as well as the flow and the pump-driving torque characteristics for various pumps for AT and CVT of vehicles have already been investigated [5], they were insufficiently analyzed. Since Wilson constructed a mathematical model for the flow and the torque characteristics in hydraulic pumps and motors [6], Schlösser [7] and Thoma [8] proposed their models based on the Wilson's model. However, their models were conceptual and have an insufficiency to represent accurately the actual characteristics of pump flow and torque. Hibi and Ichikawa [9], then, proposed an improved model for the friction torque characteristics with a non-linear change against pump speed, and the author proposed a model for the friction torque, which was based on the Hibi-Ichikawa model and took oil temperature into consideration [10].

In addition, because the model for the pump flow proposed by Wilson, Schlösser or Thoma represented inaccurately the actual pump flow, the author proposed also a model for the leakage flow which took into consideration that the thickness of clearances changed according to pressures [11]. And it was revealed that the model represented the flow characteristics accurately in various pumps. These models enable to analyze mathematically the influence of the operating conditions on the pump efficiencies. In order to improve the efficiency of the transmission for fuel economy, it would be one of the good methods for that the pump operates under a good condition of high pump efficiencies. The effectiveness of calculation using the mathematical model is validated by comparing the calculated values with the experimental ones estimated from the actually measured pump flow and torque [12].

In this study, based on the analyzed results, it is clarified how the pump efficiencies depend on the pump-operation conditions, especially oil temperature.

2. Test pumps

In this study, two types of pumps were investigated. **Figure 1** shows a cross-sectional view of pump A, which is an internal gear pump composed of an inner rotor with external gear teeth, an outer rotor with internal gear teeth, a body holding both the rotors, a cover and a stator shaft supporting the inner rotor via a bush bearing. The dimensions of pump A are presented in **Fig. 2**.

Figure 3 shows a cross-sectional view of pump B, a balanced vane pump with a fixed-displacement. It is composed of a cam ring with an elliptic inner bore, a rotor with a series of radially disposed vanes, two side plates located on both sides of the rotor and a shaft. The dimensions of pump B are presented in **Fig. 4**.

3. Experimental apparatus

Figure 5 shows a schematic diagram of the experimental system for measuring flow rate out of the pump and pump driving torque. The test pump was driven by a variable speed electric motor. The delivery pressure regulated with a throttle vale, p_d, and suction pressure, p_s, were measured at the outlet and inlet of the pump, respectively. The pressure differential across the pump Δp was defined by subtracting p_s from p_d. The oil temperature θ was measured at the pump outlet. The pump flow rate Q was measured with a gear type flow meter. In this study, by setting pump speed N and oil temperature θ at a measuring point, Q and T were measured in the process to increase p_d and to decrease it again. The mean values

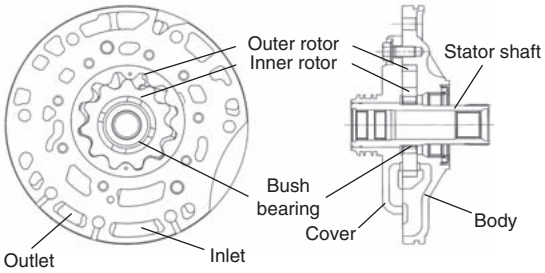

Fig. 1 Cross-sectional view of pump A

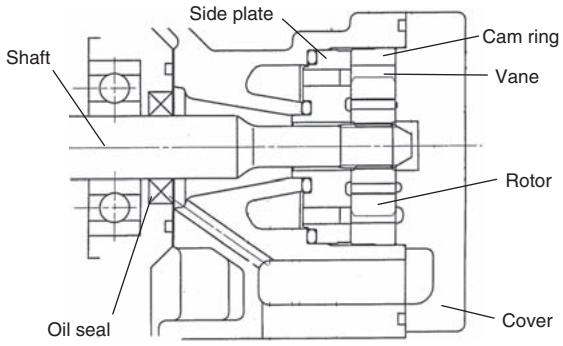

Fig. 3 Cross-sectional view of pump B

Inner rotor with external gear	External diameter of external gear	D_{e1}	(mm)	69.8
	Internal diameter of external gear	D_{i1}	(mm)	57.2
	Number of teeth	z_1		11
Outer rotor with internal gear	External diameter of internal gear	D_{e2}	(mm)	63.7
	Internal diameter of internal gear	D_{i2}	(mm)	76.3
	Number of teeth	z_2		12
	Outer diameter	D_o	(mm)	85.2
Width of rotors		b	(mm)	11.0
Inner diameter of rotor bush		D_b	(mm)	31.5
Theoretical pump displacement		V_{th}	(cm^3/rev)	13.0

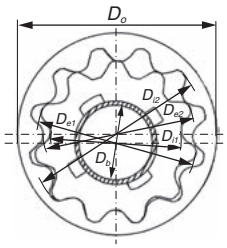

Fig. 2 Dimensions of pump A

Cam ring small radius	R_1	(mm)	18.85
Cam ring large radius	R_2	(mm)	22.32
Rotor radius	R_r	(mm)	18.55
Rotor width	b	(mm)	12.0
Vane thickness	w	(mm)	1.40
Number of vanes	z		10
Theoretical pump displacement	V_{th}	(cm^3/rev)	9.44

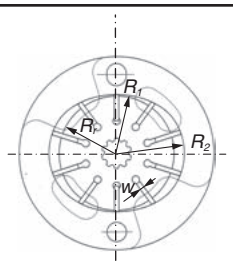

Fig. 4 Dimensions of pump B

of the two measured Q and T values were adopted as Q and T in this study. The hydraulic fluid is commercial mineral oil for CVT transmission, and its properties are given in **Table 1**.

Table 1 Properties of oil

Temperature θ (℃)	20	40	60	80	100	120	140
Density ρ (kg/m^3)	843	834	822	810	798	786	774
Viscosity μ (Pa·s)	0.0550	0.0254	0.0140	0.0085	0.0056	0.0040	0.0029

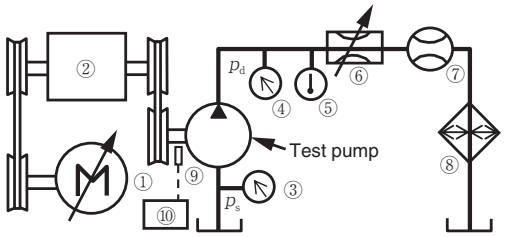

①DC variable speed electric motor 22 kW
②Torque meter (magnetostriction type) max: 50 N·m, accuracy: ±0.14 N·m
③Pressure gauge (strain gauge type) ±0.1～0 MPa, accuracy: ±0.005 MPa
④Pressure gauge (strain gauge type) 0～10 MPa, accuracy: ±0.01 MPa
⑤Thermister thermometer accuracy: ±0.1℃
⑥Flow control valve
⑦Flow meter (gear type) 1～300 L/min, accuracy: 4 cm^3/pulse
⑧Oil temperature controller (heater and cooler)
⑨Electro-magnetic sensor (measurement of pump revolution)
⑩Counter

Fig. 5 Experimental system

4. Experimental results and discussion

4. 1 Flow characteristics and its mathematical model

First, relationships between the pressure differential Δp and the flow rate Q for various pump speeds N and oil temperatures θ in tested pumps are shown in **Fig. 6**. In both the pumps, Q decreases with an increase in Δp and the decreasing slope of Q against Δp becomes greater with rising of oil temperature θ. Comparing both the pumps, the change in Q against Δp is linear in pump B shown in **Fig. 6(b)**, and is non-linear in pump A shown in **Fig. 6(a)**.

To investigate in detail, the leakage flow characteristics for these pumps are effective. The leakage flow ΔQ is obtained by subtracting the actual pump flow rate Q from the ideal flow rate Q_{th} as follows.

$$\Delta Q = Q_{th} - Q \tag{1}$$

As seen from **Fig. 7**, ΔQ is independent of N and depends on oil temperature θ (the viscosity of oil μ) and Δp. In the case of pump A, the increasing rate of ΔQ becomes greater with an increase in Δp, whereas ΔQ in pump B increases a constant rate against Δp. On the basis of the experimental data, a mathematical model for the leakage flow characteristics will be introduced. The leakage flow ΔQ* in the mathematical model for leakage flow proposed by Schlösser [7] is expressed by the following equation. In this study, because a loss flow

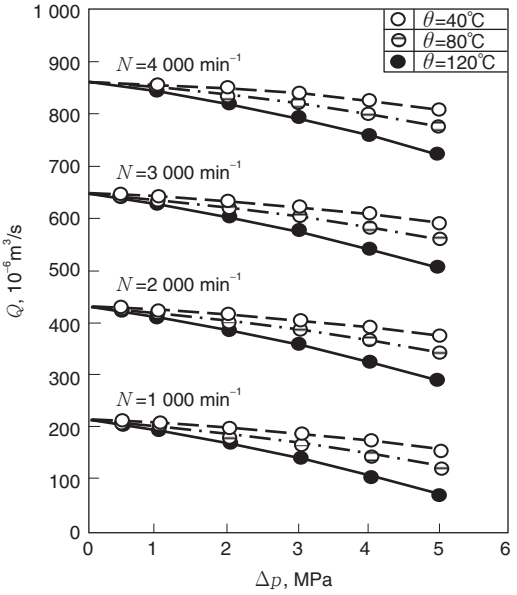

(a) Pump A (internal gear)

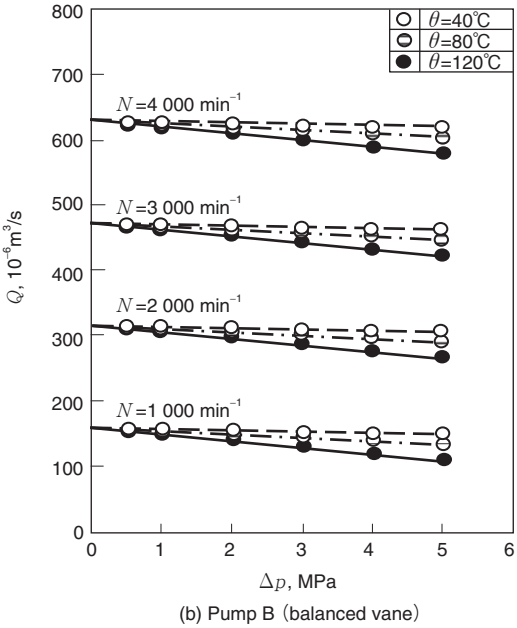

(b) Pump B (balanced vane)

Fig. 6 Flow characteristics of test pumps

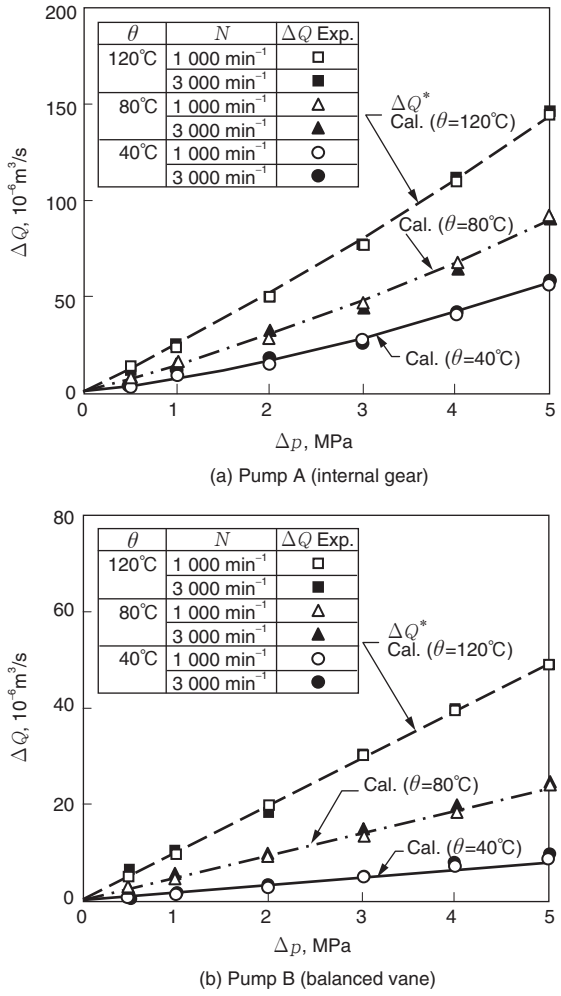

Fig. 7 Leakage flow characteristics in test pumps

due to cavitaion is not taken into account, this effect was removed from the Schlösser's model

$$\Delta Q^* = \frac{C_1}{\mu}\Delta p + \frac{C_2}{\sqrt{\rho}}\Delta p^{1/2} \quad (2)$$

Removing the second term proportional to $\Delta p^{1/2}$, the equation becomes the model of Wilson [6] or Thoma [8]. In the model proposed by Wilson [6] and that by Thoma [7], it is considered that the leakage flow ΔQ is proportional to the pressure differential Δp. This conception cannot explain the non-linear Δp–ΔQ characteristics in pump A. The Schlösser's model [7] added the component of the orifice flow leakage proportional to the square root of Δp to the Wilson's model, but cannot also explain the Δp–ΔQ characteristics of pump A, in which the increasing rate of the leakage flow against Δp becomes greater and greater with an increase in Δp.

Therefore, the author proposed a new model for the leakage flow ΔQ, in which the thickness of the clearance causing the leakage changed according to the pressure differential Δp. As a result, the model was able to represent the Δp–ΔQ characteristics under various pump-operating conditions, such as pressures, pump speeds and oil temperatures for various types of pumps. The model used is as follows:

$$\Delta Q^* = \frac{C_a}{\mu}\Delta p + \frac{C_b}{\mu}\Delta p^2 + \frac{C_c}{\sqrt{\rho}}\Delta p^{1/2} + \frac{C_d}{\sqrt{\rho}}\Delta p^{3/2} \quad (3)$$

where C_a to C_d are pump constants according to the exponent of Δp, μ is the viscosity of oil and ρ is the density of oil. The derivation of equation (3) is described in the reference [11]. The terms on the right-hand side of equation (3) mean from the left as follows: the first term dependent on Δp is the viscous flow leakage through the initial clearance in parts like parallel disks or plates, the second term dependent on Δp^2 is the changed viscous flow leakage due to the change in the clearance in parts like the parallel disks or plates, the third term dependent on $\Delta p^{1/2}$ is the orifice flow leakage through the initial clearance, and the fourth term dependent on $\Delta p^{3/2}$ is the changed orifice flow leakage due to the change in the clearance. The first and second terms have an inverse of μ, and the third and fourth terms have that of $\sqrt{\rho}$ and are independent of μ. In the case of C_c=C_d=0, equation (3) becomes the Schlösser' model, and furthermore by setting C_b=0 it results in the Wilson's model.

All the constants of C_a to C_d for the leakage flow in **Table 2** were estimated from the actual Δp–ΔQ characteristics in both the test pumps. Substituting the values in **Table 2** for C_a to C_d in equation (3), ΔQ against Δp can be calculated for each oil temperature. The calculated leakage flow using the mathematical model is expressed as ΔQ* with comparison toΔQ experimented.

Figure 7 shows the comparisons between ΔQ experimented and ΔQ* calculated for three oil temperatures. As seen from this figure, ΔQ* accurately agrees with ΔQ and the mathematical model can well represent also non-linear Δp–ΔQ characteristics in pump A.

Table 2 Values of pump constants for leakage flow in test pumps

	C_a (m³)	C_b (m⁵/N)	C_c (m²)	C_d (m²/N)
Pump A (Internal gear)	8.73×10^{-14}	0	2.73×10^{-9}	1.03×10^{-13}
Pump B (Balanced vane)	3.93×10^{-14}	0	0	0

4. 2 Torque characteristics and its mathematical model

Next, the characteristics of the pump driving torque T in pumps A and B were investigated and their results are shown in **Fig. 8**. The conditions of Δp=1, 2 and 5 MPa are chosen because the transmissions are mostly operated nearby at 1 MPa, the maximum operating pressure of AT is 2 MPa and that of CVT is 5 MPa. Also the torque characteristics and the pump efficiencies are investigated and evaluated at these pressure differentials.

In contrast to the flow characteristics, the torque characteristics have a complex configuration affected by pump-operating conditions such as the pump speed N, the operating pressure differential Δp and oil temperature θ. In order to understand the torque characteristics in detail, the relationship between N and the friction torque ΔT should be investigated. The friction torque ΔT is obtained by subtracting the ideal torque T_{th} from the pump driving torque T, as expressed by the following equation.

$$\Delta T = T - T_{th} \tag{4}$$

Figure 9 shows the relationships between N and ΔT for three kinds of Δp and θ in pumps A and B. Although ΔT varies complicatedly according to N, Δp and θ, ΔT increases with an increase in Δp in all cases of θ. When Δp is low, ΔT has a nearly monotonous increase with an increase in N. In contrast, ΔT decreases first and then increases with an increase in N when Δp becomes higher for all cases of θ. This change appears remarkably with increasing θ. Pump B has the characteristic similar to that of pump A.

The mathematical model for friction torque was originally proposed by Wilson [6] through his excellent concept that the friction torque consists of three components: (1) a component dependent on the friction proportional to the pressure, (2) a component dependent on the viscous friction due to oil shearing concerning the pump speed and the viscosity of fluid, and (3) a component independent of pump-operating conditions. The friction torque of his model is expressed as ΔT^* by the following equation.

$$\Delta T^* = C_f V_{th} \Delta p + C_n \mu V_{th} \omega + T_c \tag{5}$$

In equation (5), C_f, C_n and T_c are constants independent of Δp, ω(=2πN/60) and oil temperature θ. However, this model cannot simulate the non-linear characteristics between N and ΔT shown in **Fig. 9**. Schlösser' proposed his model [7] adding a component proportional to the product of the mass of oil and the square of the pump speed to the Wilson' model, but it cannot also represent such characteristics. Hibi and Ichikawa [8] proposed a new model, in which the pump constant C_f in the Wilson' model was treated as a function of the pump angular velocity ω. Although their model can represent the

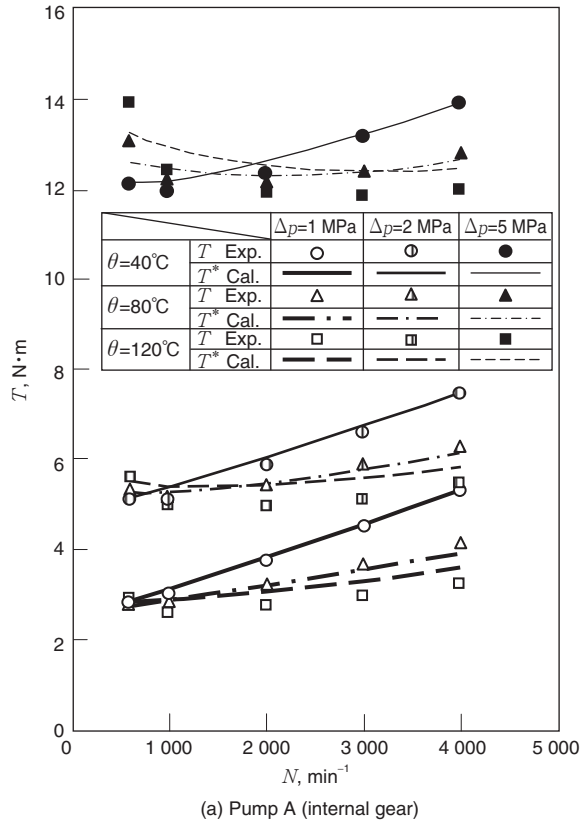

(a) Pump A (internal gear)

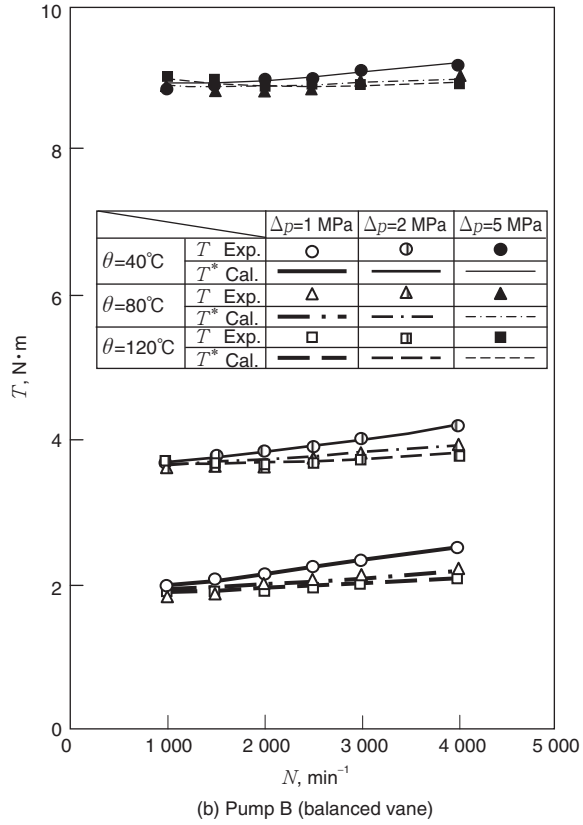

(b) Pump B (balanced vane)

Fig. 8 Pump driving torque characteristics in test pumps

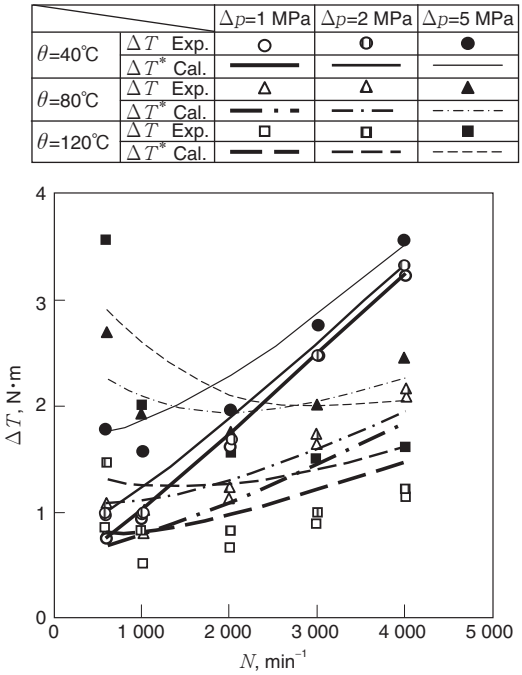

(a) Pump A (internal gear)

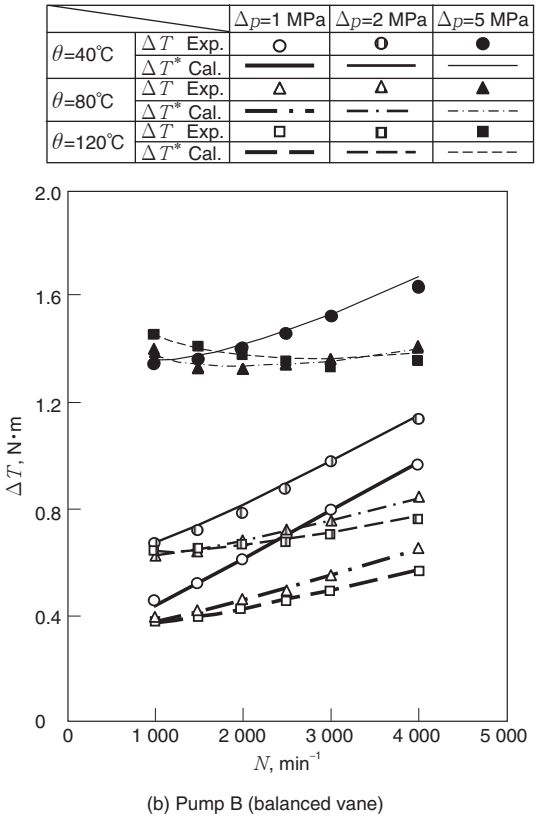

(b) Pump B (balanced vane)

Fig. 9 Friction torque characteristics in test pumps

non-linear characteristics between N and ΔT, it was insufficient in consideration of oil temperature. Therefore, the author proposed an improved model adding a factor regarding oil temperature to the component dependent on Δp and another factor independent of the viscosity of oil to the component dependent on ω in the model of Hibi and Ichikawa [10].

$$\Delta T^* = \frac{C_{f0}V_{th}}{1+(\omega/\omega_o)^{\alpha}}\left\{1+C_\theta\frac{\theta-\theta_o}{\theta_o}\right\}\Delta p + (C_g\mu + C_h)V_{th}\omega + T_c \quad (6)$$

where coefficients in equation (6) such as C_{f0}, ω_0, α, C_θ, θ_0, C_g, C_h and T_c are pump constants for friction torque characteristics independent of pump-operating conditions of $\omega(=2\pi N/60)$, θ, Δp and μ. The values of these constants are determined from the experimental data of T and presented in **Table 3** for two pumps tested in this study. The pump driving torque is calculated as T^* by adding the ideal torque $T_{th}=V_{th}\Delta p/(2\omega)$ to ΔT^* in equation (6). The changes in T^* and ΔT^* calculated using equation (6) and the values in **Table 3** are indicated with various lines, respectively. Comparing ΔT^* with ΔT in **Fig. 9**, the mathematical model can not exactly represent the changes in ΔT in a region of low N at a high oil temperature for pump A. However, it can be seen that T for actual pumps A can be well estimated by using the mathematical model under various pump-operating conditions, as seen from **Fig. 8**.

5. Influence of oil temperature on pump efficiencies

5. 1 Volumetric efficiency

In this study, the volumetric efficiency denoted using the actual flow rate η_v and that denoted using the leakage flow calculated from equation (3) η_v^* are expressed as follows.

$$\eta_v = \frac{Q}{Q_{th}} = \frac{(Q_{th}-\Delta Q)}{Q_{th}} \quad (7)$$

$$\eta_v^* = \frac{(Q_{th}-\Delta Q^*)}{Q_{th}} \quad (8)$$

Figure 10 shows the relationships between the pump speed N and the volumetric efficiency for three Δp of 1, 2 and 5 MPa at oil temperature of 80℃. In **Fig. 10**, the volumetric efficiency of pump B is higher than that of pump A and η_v^* agree well with η_v in both the pumps.

Table 3 Values of pump constants for friction torque in test pumps

	C_{fo}	ω_o (rad/s)	α	C_θ	θ_o (℃)	C_g	C_h (Pa・s)	T_c (N・m)
Pump A (internal gear)	0.2376	170.3	1.413	0.7202	80	0.1016	1.093×10^{-3}	0.015
Pump B (balanced vane)	0.2669	329.6	0.456	0.1682	80	0.0326	4.410×10^{-4}	0.004

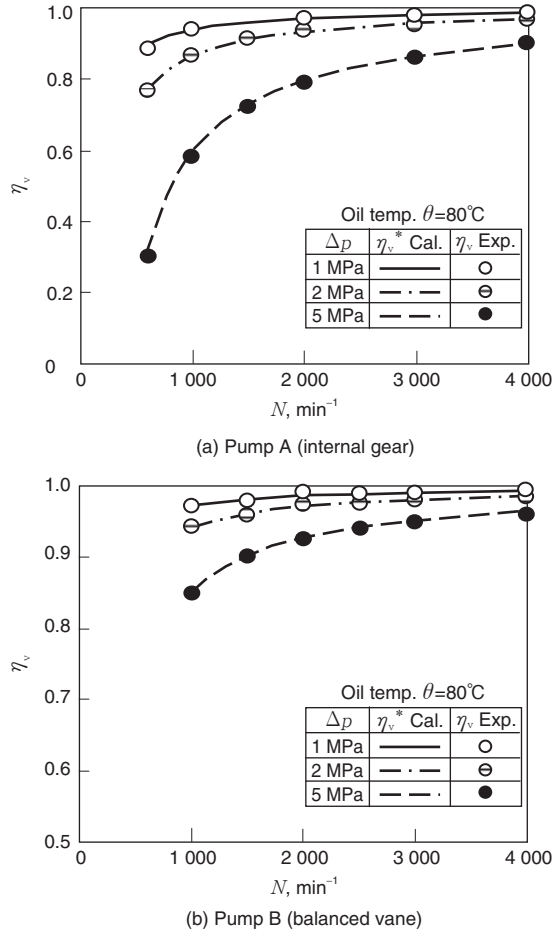

Fig. 10 Changes in volumetric efficiency in test pumps

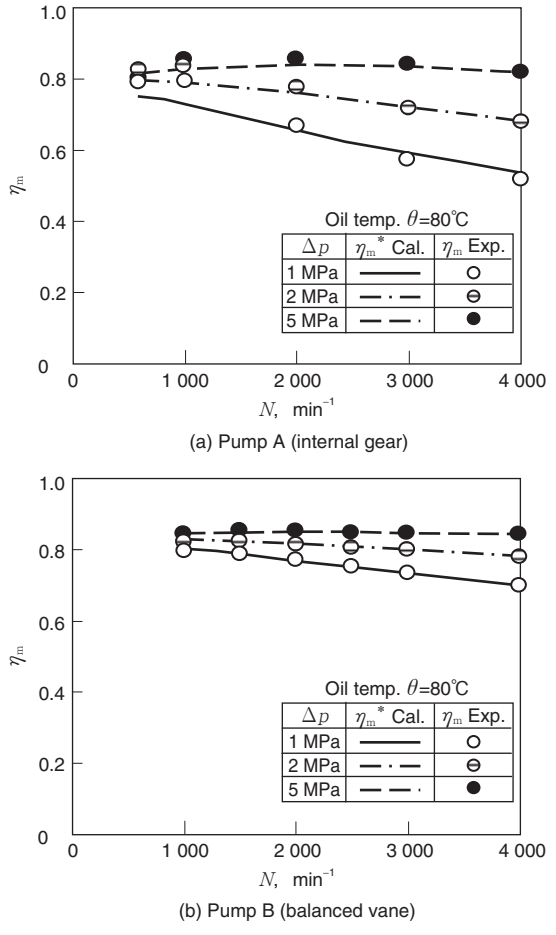

Fig. 11 Changes in mechanical efficiency in test pumps

5. 2 Mechanical efficiency

Similarly to the volumetric efficiency, the mechanical efficiency denoted using the actual pump driving torque η_m and that denoted using the friction torque calculated from equation (6) η_m* are expressed as follows.

$$\eta_m = \frac{T_{th}}{T} = \frac{T_{th}}{T_{th} + \Delta T} \tag{9}$$

$$\eta_m^* = \frac{T_{th}}{T_{th} + \Delta T^*} \tag{10}$$

Figure 11 shows the changes in the mechanical efficiency against the pump speed N for aforementioned Δp at θ=80℃. For the mechanical efficiency, η_m* using ΔT* calculated from equation (6) agrees well with η_m obtained from the actual pump driving torque T.

5. 3 Overall efficiency

Finally, two overall efficiencies η and η* are denoted as the product of η_v and η_m obtained from measured T and Q and that of η_v* and η_m* calculated using the mathematical models for ΔQ* and ΔT*, respectively.

$$\eta = \eta_v \eta_m \tag{11}$$

$$\eta^* = \eta_v^* \eta_m^* \tag{12}$$

Figure 12 shows the changes in the overall efficiency against the pump speed N for three kinds of Δp at θ=80℃. In the case of pump A shown in **Fig. 12(a)**, the change in the overall efficiency against N as well as Δp is large. In contrast, pump B has a small change in the overall efficiency against N and Δp, as shown in **Fig.12(b)**. In both the pumps, η* agrees well with η through all the measured conditions.

Figure 13 shows the influence of oil temperature θ on the overall efficiency for various kinds of N and Δp. Both the pumps have similar changes in the overall efficiency. In the range of θ from 20℃ and 140℃, with decreasing N, the overall efficiency increases at a lower Δp of 1 MPa and decreases at a higher Δp of 5 MPa. In this figure, the agreement of η* with η is excellent.

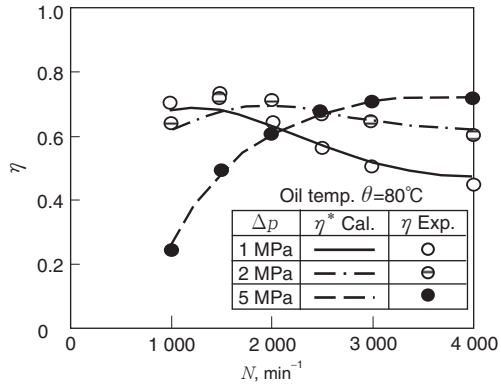

(a) Pump A (internal gea)

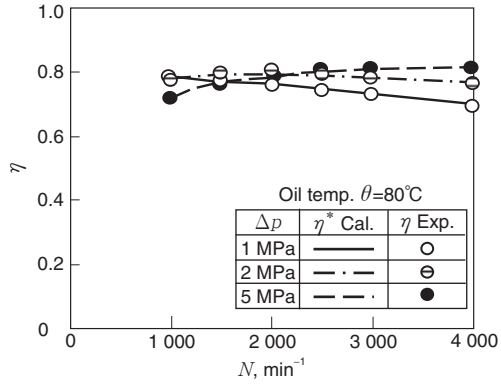

(b) Pump B (balanced vane)

Fig. 12 Changes in overall efficiency in test pumps

A hydraulic pump for a vehicle operates under various conditions of N, Δp and θ. Therefore, it would be important to understand the actual overall efficiency of the pump. Then, the overall efficiency η^* calculated using the mathematical models for the leakage flow and the friction torque was plotted on the θ–N plane for three kinds of Δp. **Figure 14** shows the result that the pumps have an area of higher overall efficiency as a whole at θ nearby 80 ℃. The increase in N prevents the overall efficiency from going down when θ becomes higher. In addition, pump operation at a higher N prevents the overall efficiency from falling down at a high oil temperature.

6. Conclusions

In this study, the influence of oil temperature on various pump efficiencies was analyzed by using mathematical models for the leakage flow characteristic and the friction torque characteristics in an internal gear and a balanced vane pumps used for an automatic transmission in a vehicle. As a result, the following conclusions were drawn.

Using the mathematical models, it could be possible to survey the pump operating conditions with higher efficiencies. Because the viscosity of oil decreased sharply with an increase in oil temperature, the volumetric efficiency fell down remarkably in the range of high oil temperature.

In contrast, the mechanical efficiency fell down remarkably in the region of a low oil temperature because

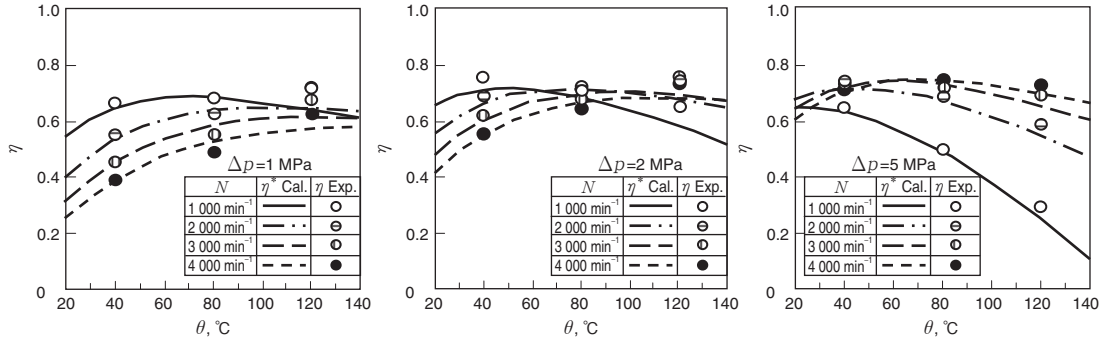

(a) Pump A (internal gear)

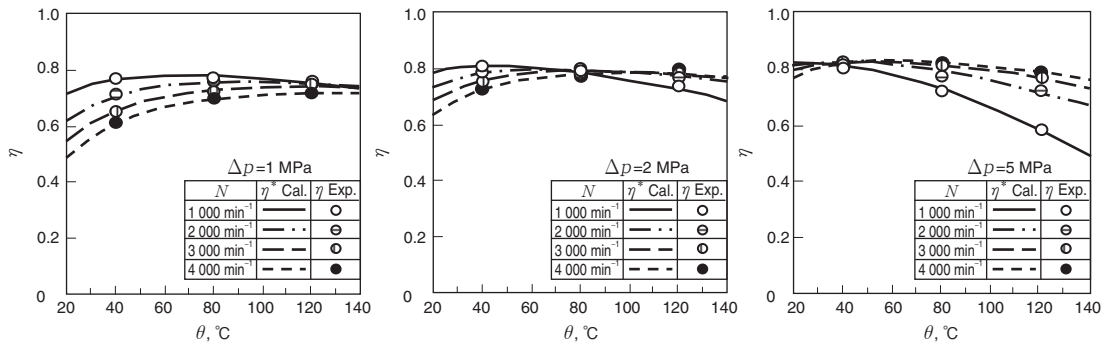

(b) Pump B (balanced vane)

Fig. 13 Changes in overall efficiency against oil temperature

the viscous friction to shear oil increased sharply. In addition, even in the range of high oil temperature, it did not increase because the friction torque dependent on the pressure differential significantly increased.

The overall efficiency obtained as the product of the volumetric and the mechanical efficiencies had a good condition in the vicinity of 80℃, and increasing or decreasing oil temperature from the vicinity worsened the overall efficiency. Also operating the pumps at a higher speed could maintain a high overall efficiency for an increase in oil temperature.

C_a : pump constant independent of pump-operating condition (m^3)
C_b : pump constant independent of pump-operating condition ($m^3/Pa=m^3/N$)
C_c : pump constant independent of pump-operating condition (m^2)
C_d : pump constant independent of pump-operating condition ($m^2/Pa=m^4/N$)
C_{fo} : pump constant independent of pump operating condition (–)
C_g : pump constant independent of pump operating condition (–)
C_h : pump constant independent of pump operating condition (Pa·s)
C_θ : pump constant independent of pump operating condition (–)
N : pump speed (r/min)
p_d : delivery pressure (MPa)
p_s : suction pressure (MPa)
Q : actual pump flow rate (m^3/s)
Q_{th} : ideal pump flow rate ($=V_{th}N/60$) (m^3/s)
T : driving torque of pump (Nm)
T_c : friction torque independent of Δp and N (Nm)
T_{th} : ideal torque of pump ($=V_{th}\Delta p$) (Nm)
V_{th} : theoretical pump displacement per radian (cm^3/rev.)
α : pump constant independent of pump operating condition (–)
Δp : pressure differential across pump ($=p_d-p_s$) (Pa)
ΔQ : total leakage flow ($=Q_{th}-Q$) (m^3/s)
ΔT : total friction torque ($=T-T_{th}$) (Nm)
η : overall efficiency ($=\eta_m+\eta_v$) (–)
η_m : mechanical efficiency ($=T_{th}/T$) (–)
η_v : volumetric efficiency ($=(Q_{th}-\Delta Q)/Q_{th}$) (–)
θ : oil temperature (℃)
μ : viscosity of oil (Pa·s)
ω : angular velocity of pump ($=2\pi N/60$) (rad/s)
ω_o : pump constant independent of pump operating condition (rad/s)
ρ : density of oil (kg/m^3)

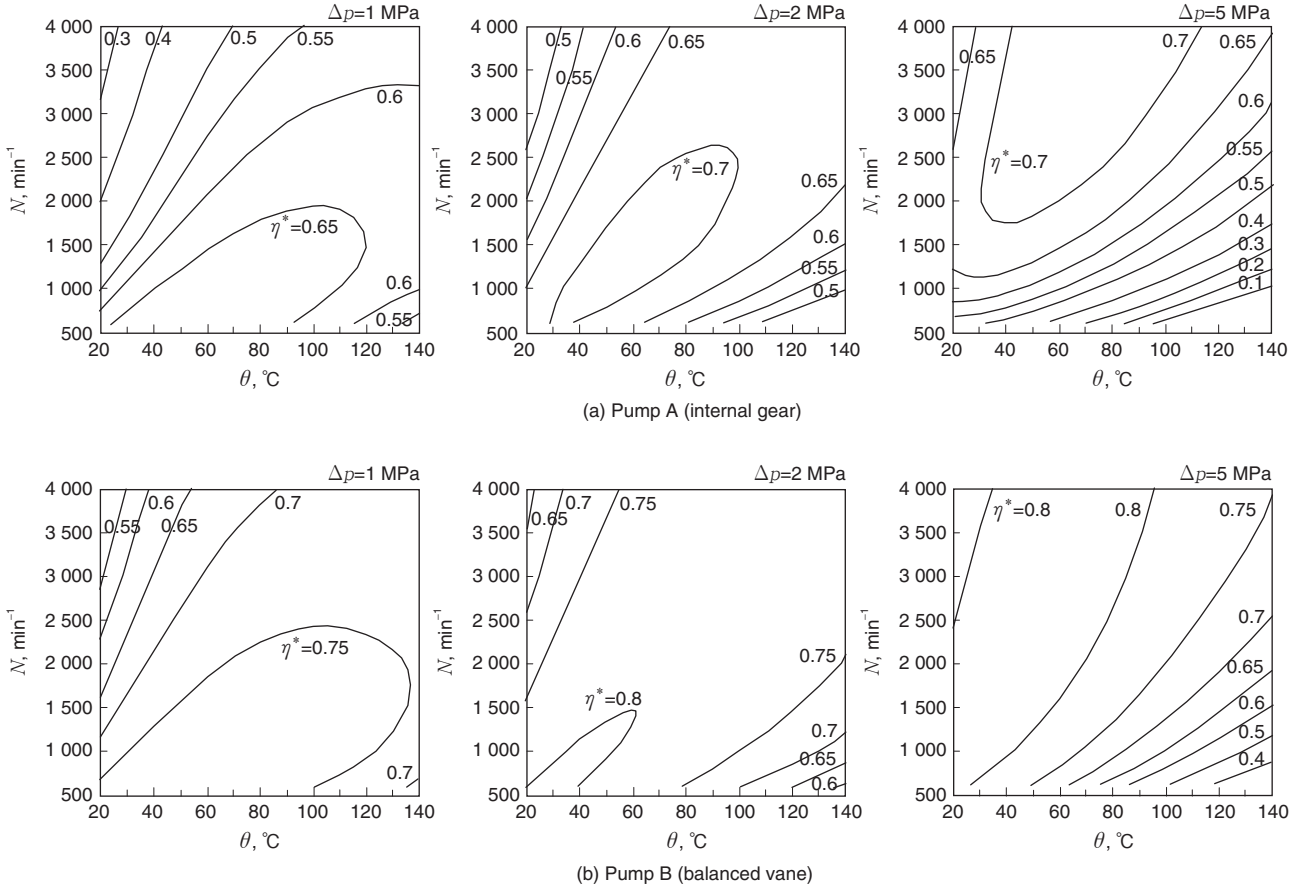

Fig. 14 Overall efficiency map in test pumps

References

1) Kanada, T., Iijima, Y., Yasue, H. and Takahashi, T.: Toyota's New Generation "Super ECT" (U-140E) Four-Speed Automatic Transaxle, SAE Paper 1999-01-0749 (1999).
2) Ozeki, T. and Umeyama, M.: Development of Toyota's Transaxle for Mini-van Hybrid Vehicles, SAE Paper 2002-01-0931 (2002).
3) Shimizu, K., Waki, H., Saito, T., Sawayama, M., Nishiyama, H., Kuroda, S. and Oohori, T.: Development of a New-Generation CVT with Medium Torque Capacity for Front-Drive Cars, SAE Paper 2006-01-1306 (2006).
4) Ide, T.: Effect of Belt Loss and Oil Pump Loss on the Fuel Economy of a Vehicle with a Metal V-Belt CVT, Proceedings of Seoul 2000 FISITA World Automotive Congress, paper no. FA200A131 (2000) 1-6.
5) Kluger, M., A., Fussner D., R. and Roethler, B.: A Performance Comparison of Various Automatic Transmission Pumping Systems", SAE Paper 960424 (1996).
6) Wilson, W., E.: Rotary-Pump Theory, Trans. ASME, vol. 68, no. 4 (1946) 371-383.
7) Schlösser, W., M., J.: Ein mathematisches Modell für Verdrängerpumpen und -motoren, Oelhydraulik und pneumatik, vol. 5, no. 4 (1961) 122-129.
8) Thoma, J., U.: Mathematische Modelle und die effective Leistung hydrostatischer Maschinen und Getriebe, ölhydraulik und pneumatic, vol. 14, no. 6 (1970) 233-237.
9) Hibi, A. and Ichikawa, T.: Mathematical Model of the Torque Characteristics for Hydraulic Motors, Bull. JSME, vol. 20, no. 143 (1977) 616-621.
10) Inaguma, Y.: Oil temperature influence on friction torque characteristics in hydraulic pumps, Proc. Inst Mech Eng, Part C: J. Mechanical Engineering Science, vol. 226, no. 9 (2012) 2267-2280.
11) Inaguma, Y.: A practical approach for analysis of leakage flow characteristics in hydraulic pumps, Proc. Inst Mech Eng, Part C: J. Mechanical Engineering Science, vol. 227, no. 5 (2013) 980-991.
12) Inaguma, Y. and Yoshida, N.: Mathematical Analysis of Influence of Oil Temperature on Efficiencies in Hydraulic Pumps for Automatic transmissions, SAE Paper 2013-01-0820 (2013).


N. YOSHIDA* Y. INAGUMA**

* *Hydraulic System Engineering Dept., Automotive Systems Business Headquarters*
** *Hydraulic System Engineering Dept., Automotive Systems Business Headquarters, Doctor of Engineering*